Electronic Supplementary Material (ESI) for Physical Chemistry Chemical Physics.

Supporting Information

Stabilization of ultra-small $[Ag_2]^{2+}$ and $[Ag_m]^{n+}$ nano-clusters through negatively charged tetrahedrons in oxyfluoride glass networks: To largely enhance the luminescence quantum yields

Ronghua Ma,[a] Junjie Zhao,[a] Xiaotong Chen,[a] Xvsheng Qiao,[a,*] Xianping Fan, [a] Jincheng Du[b] and Xianghua Zhang [c]

[a] *State Key Laboratory of Silicon Materials & School of Materials Science and Engineering, Zhejiang University, Hangzhou 310027, China*

[b] *Department of Materials Science and Engineering, University of North Texas, Denton, Texas 76203-5017, U.S.*

[c] *Laboratory of Glasses and Ceramics, Institute of Chemical Science UMR CNRS 6226, University of Rennes 1, 35042 Rennes, France*

* Corresponding author. E-mail: qiaoxus@zju.edu.cn; Tel.: +86-571-87951234.

Table S1 The external quantum efficiencies (EQE) and the internal quantum efficiencies (IQE) of the glass samples with excitation at 280 and 330 nm. Here the luminescent external quantum efficiencies (EQE) were harshly estimated by further considering the optical absorptance of the sample at excitation wavelength. The absorptance is evaluated by the ratio of the sample absorption devided by the input lamp source intensity.

Sample	Ex 280 nm		Ex 330 nm	
	IQE	EQE	IQE	EQE
G1	34.9%	25.6%	30.9%	7.2%
G2	38.3%	26.2%	36.2%	9.1%
G3	62.7%	46.6%	63.9%	32.2%
G4	89.7%	79.8%	73.7%	48.8%
G5	81.2%	74.0%	64.6%	36.7%

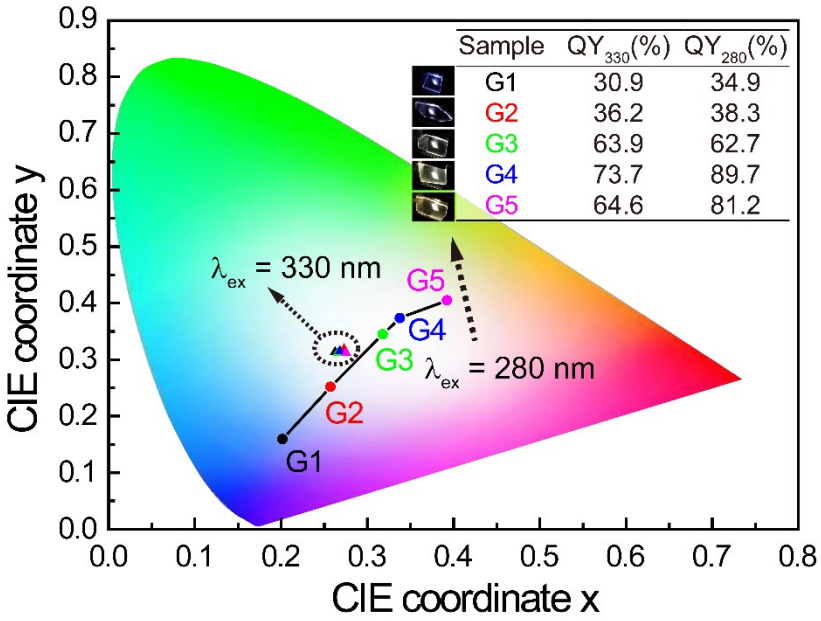

Fig. S1 CIE chromaticity coordinates of G1-5 emission under excitations at 280 nm and 330 nm. The inset table lists the related quantum yields and the inset luminescence photographs of G1-5 are under irradiation of Xe-lamp (280 nm).

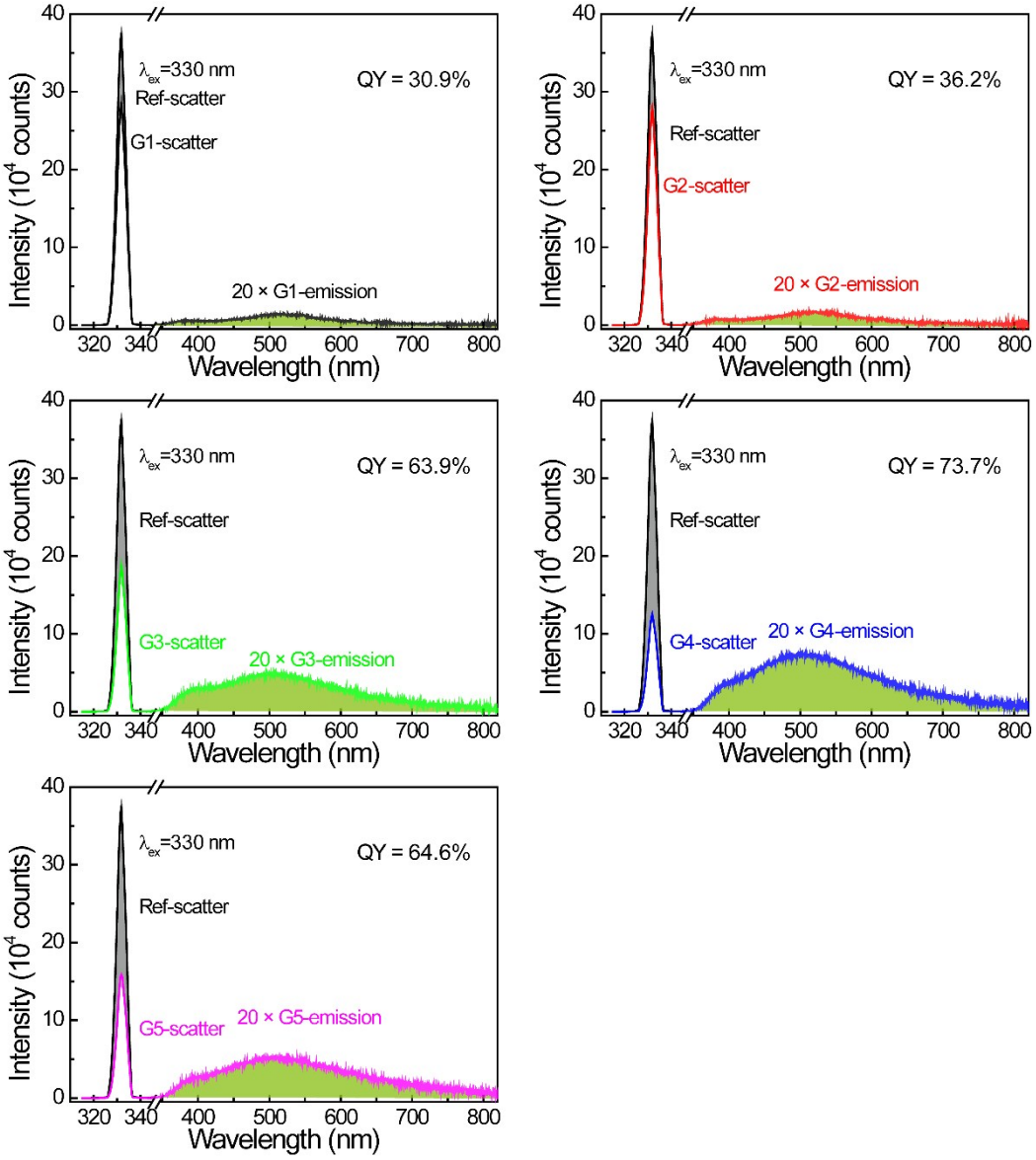

Fig. S2 Spectra of internal quantum yield measurements (scatter range on the left and emission range on the right) for G1-5 under 330 nm excitation.

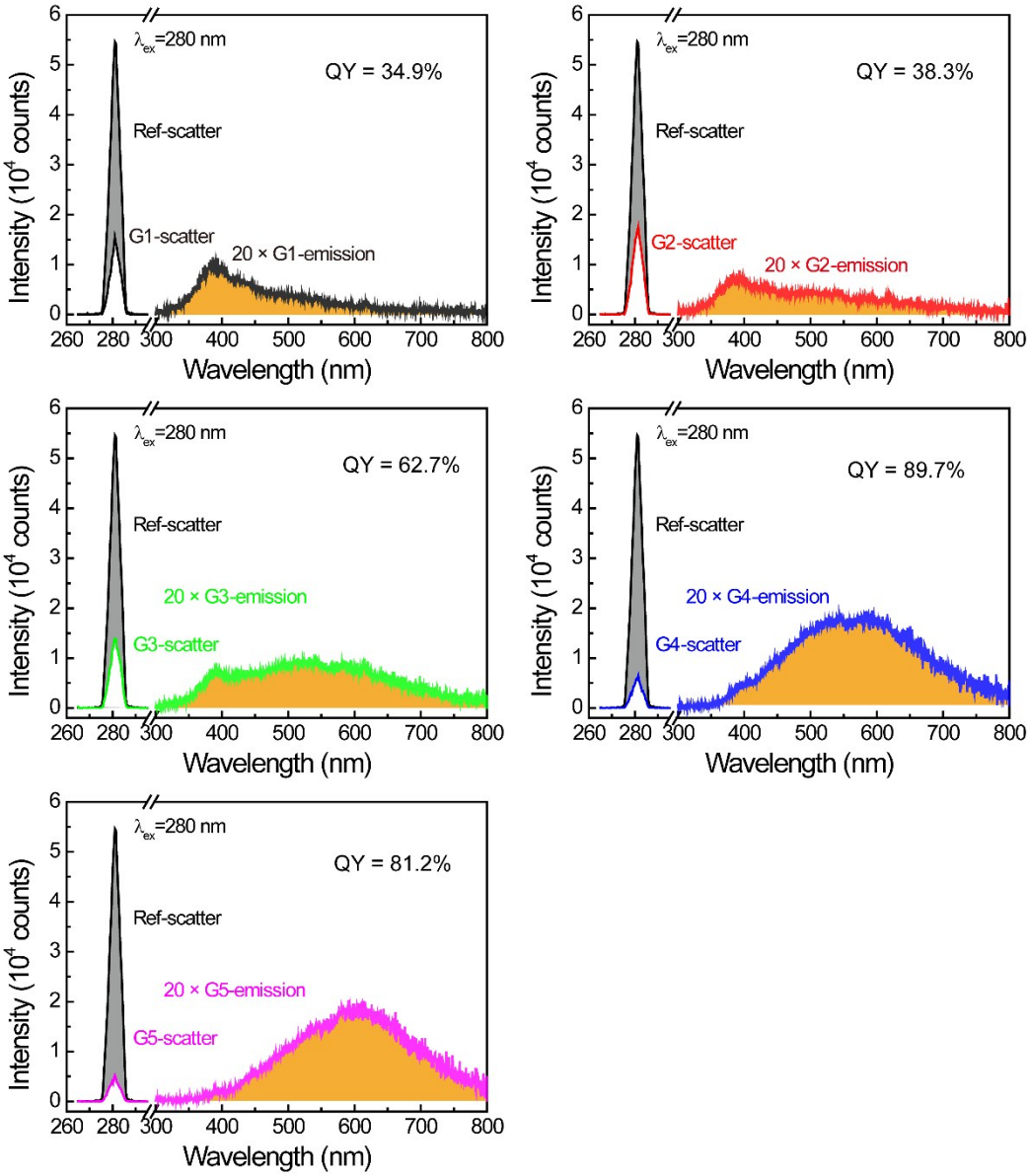

Fig. S3 Spectra of internal quantum yield measurements (scatter range on the left and emission range on the right) for G1-5 under 280 nm excitation.

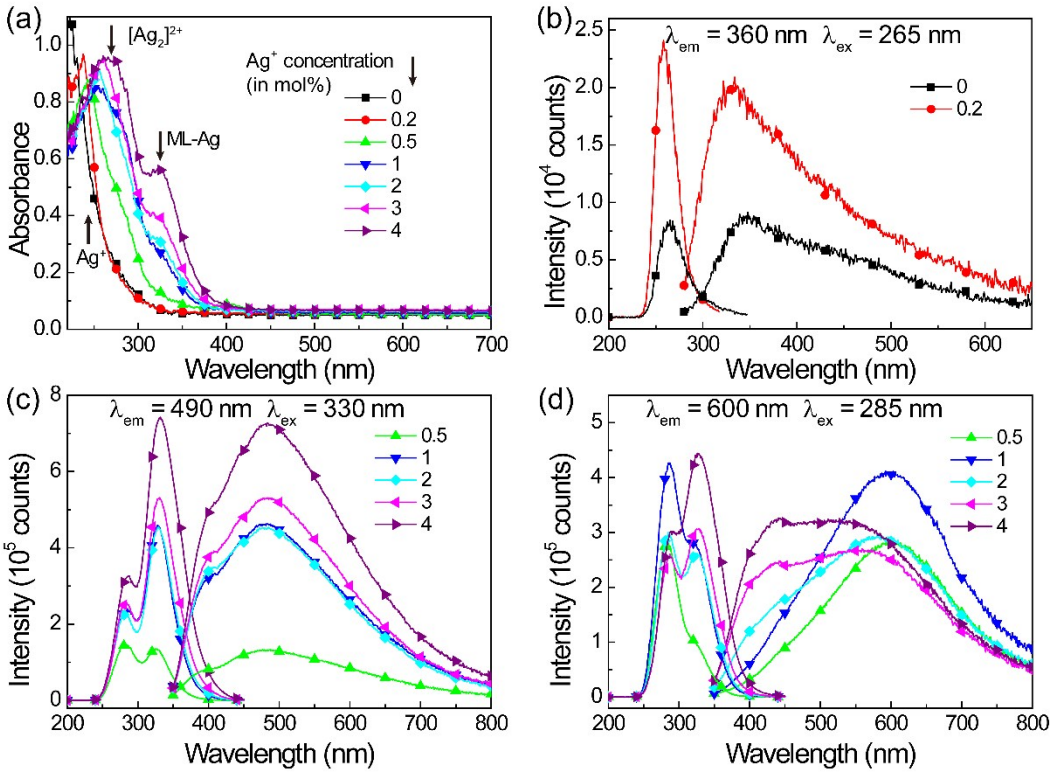

Fig. S4 Spectroscopic investigation on the glasses with different silver concentrations: **(a)**optical absorption spectra; **(b-d)** PL excitation and emission spectra with monitoring and excitation at the feature wavelengths corresponding to Ag^+, ML-Ag and $[Ag_2]^{2+}$, respectively. The glass compositions are $55SiO_2$-$10Al_2O_3$-$10ZnF_2$-$15CaF_2$-$10B_2O_3$-$xAgNO_3$ (x =0, 0.2, 0.5, 1, 2, 3, 4 in mol%).

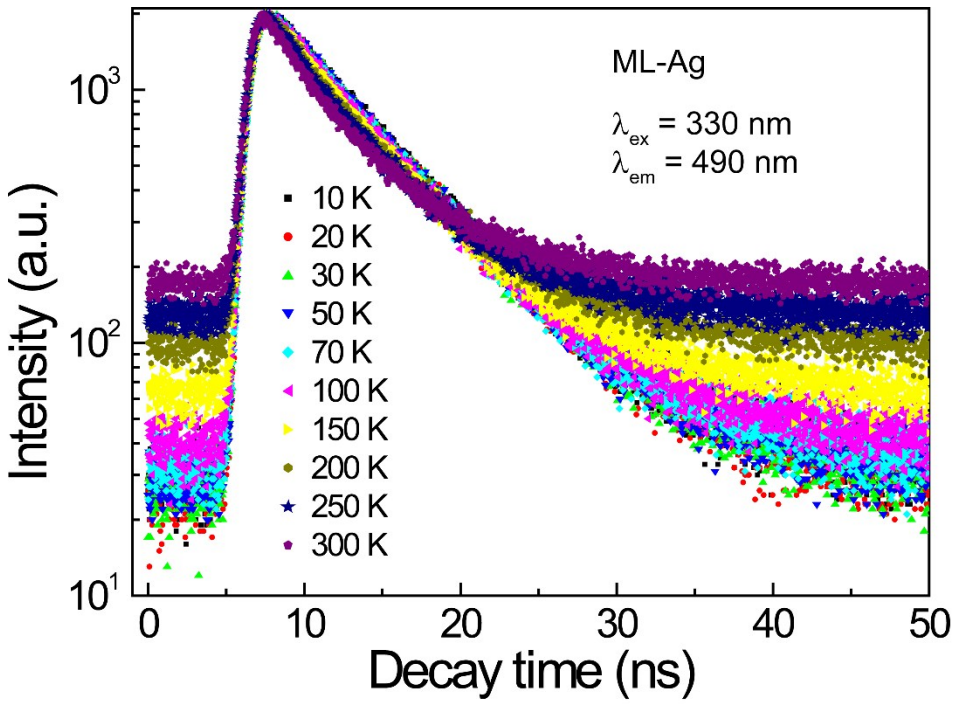

Fig. S5 Temperature dependent PL decay curves of the silver doped glass with monitoring at 490 nm and excitation at 330 nm: A fast decay within nanoseconds and slow decay within microseconds which forms the baseline here.

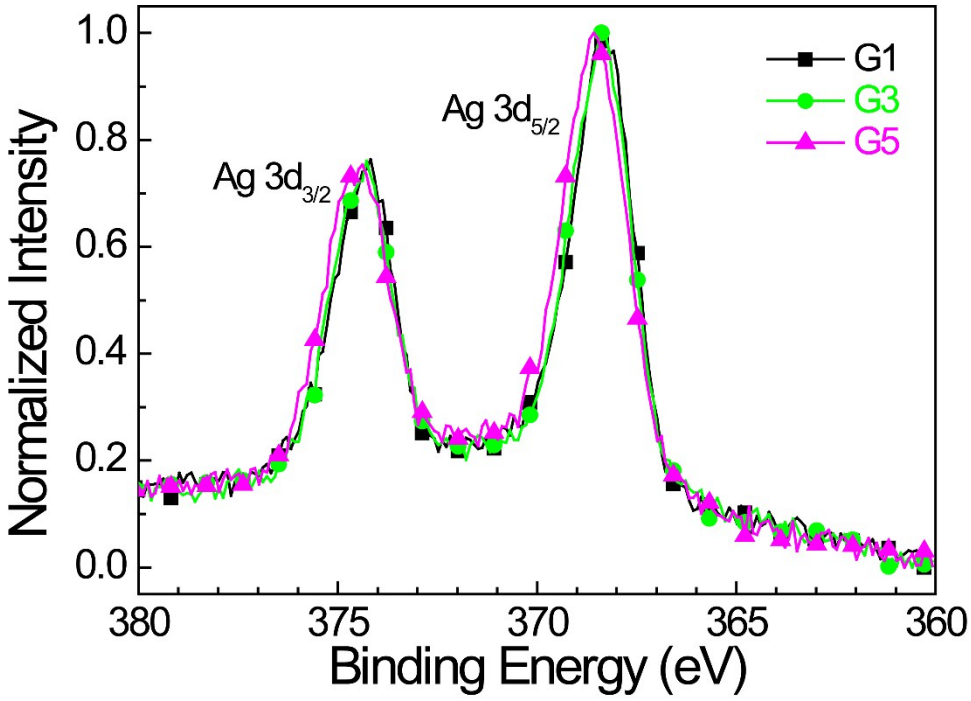

Fig. S6 Normalized Ag 3d X-ray photoelectron spectra (XPS) spectra of G1, G3 and G5. The tiny shift in binding energy is due to the change in Ag^{+} doping environment and the reduction of Ag^{+} in different degree.

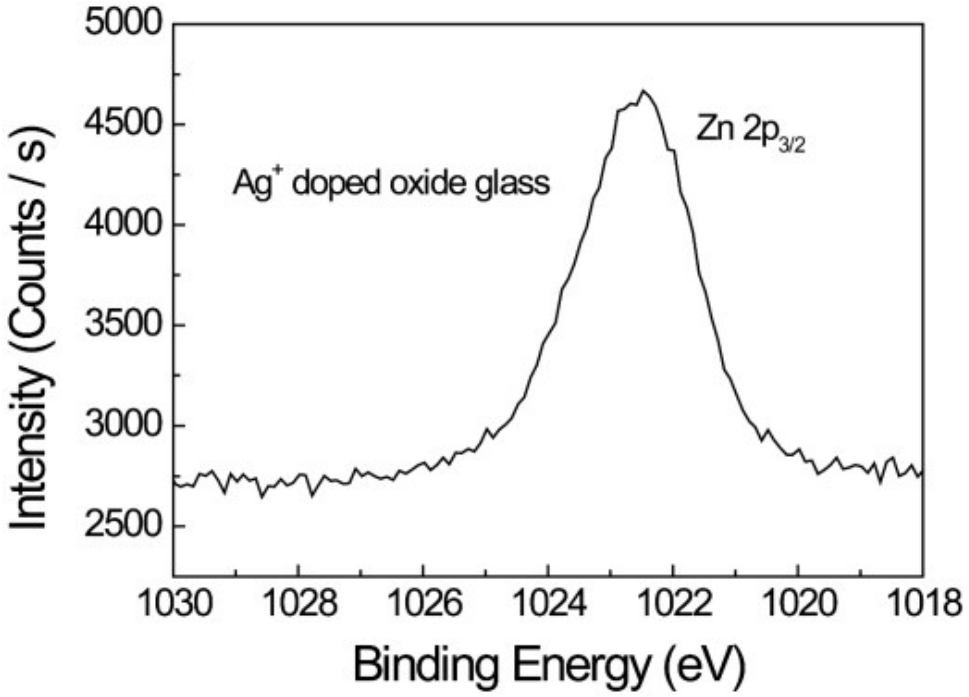

Fig. S7 Zn 2p X-ray photoelectron spectra (XPS) spectra of the SiO_2-Al_2O_3-ZnO-CaO-B_2O_3-Ag_2O glass.